



Full prediction of unsaturated hydraulic conductivity - comparison of four different capillary bundle models

Andre Peters^{1*}, Sascha C. Iden¹, and Wolfgang Durner¹

¹Division of Soil Science and Soil Physics, Institute of Geoecology, Technische Universität Braunschweig, Germany

Correspondence to: Andre Peters (a.peters@tu-braunschweig.de)

Abstract. To model the water, solute and energy transport in porous media, it is essential to have accurate information about the soil hydraulic properties (SHP), i.e. the water retention curve (WRC) and the soil hydraulic conductivity curve (HCC). Having reliable data information to parameterize these models is important, but equally critical is the selection of appropriate SHP models. While various expressions for the WRC are commonly compared, the capillary conductivity model proposed by Mualem (1976a) is widely used but seldom compared to alternatives. The objective of this study was to compare four different capillary bundle models in terms of their ability to accurately predict the HCC without scaling the conductivity function by a measured conductivity value. These expressions include two simpler models proposed by Burdine (1953) and Alexander and Skaggs (1986), which assume a bundle of parallel capillaries with tortuous flow paths, and two more sophisticated models based on statistical cut-and-random-rejoin approaches, namely those proposed by Childs and Collis-George (1950) and the aforementioned model of Mualem (1976a). In order to check whether different parametrizations of the WRC interfere with the suitability of the conductivity models, we utilized four different capillary saturation models in combination with each of the conductivity prediction models, resulting in a total of 16 SHP model schemes. All schemes were calibrated using 12 carefully selected datasets that provided water retention and hydraulic conductivity data over a wide saturation range. Subsequently, the calibrated models were tested and rated by their ability to predict the hydraulic conductivity of 23 independent datasets of soils with varying textures. The statistical cut-and-random-rejoin models, particularly the Mualem (1976a) model, outperformed the simpler capillary bundle models in terms of predictive accuracy. This was independent of the specific WRC model used. Our findings suggest that the widespread use of the Mualem model is justified.

1. Introduction

Representing the soil hydraulic properties in functional form is mandatory for simulation of water, energy and solute transport in the vadose zone. The most established models for the WRC (e.g. van Genuchten, 1980, or Kosugi, 1996) and the HCC (e.g. Burdine, 1953 or Mualem, 1976a) account for water storage and flow in capillaries but neglect water flow and adsorption in films and corners. The latter effects become, however, dominant if the soils get dry. Therefore, more recent



models extend these SHP models (e.g. Tuller and Or, 2001; Peters and Durner, 2008, Lebeau and Konrad, 2010; Zhang, 2011; Peters, 2013) to account for these processes. In the very dry range, any liquid flow ceases and vapor flow becomes the dominant transport process. If the water transport is approximated as isothermal, vapor conductivity might be predicted on
35 basis of the retention function and directly incorporated into an effective total conductivity function (Peters and Durner, 2010).

The current models used to predict the HCC, which include both capillary and non-capillary components, do not fully predict the hydraulic conductivity $K(h)$, but require scaling of a relative conductivity function using measured data. Indeed, both the capillary conductivity and the film and corner flow conductivity must be scaled in some of these models (Peters, 2013). This
40 approach is unsatisfactory as data in the relevant moisture range may be missing (particularly in the dry range) or unreliable (if saturated conductivity is dominated by soil structure), leading to considerable uncertainties in the HCC. To overcome these shortcomings, Peters et al. (2021) proposed a simple yet physically based prediction scheme for the absolute non-capillary conductivity by combining the physically based models for film flow proposed by Lebeau and Konrad (2010) and Tokunaga (2009) with the empirical Peters–Durner–Iden (PDI) model developed by Peters (2013; 2014) and Iden and Durner
45 (2014). In a recent study, Peters et al. (2023) further enhanced the HCC prediction from the WRC by an prediction of the absolute capillary conductivity component using the Mualem (1976a) capillary bundle model. This extended approach allows for a conductivity prediction that covers the entire moisture range from near saturation to oven dryness, and overcomes the limitations associated with missing or unreliable conductivity data in the relevant moisture range.

A multitude of capillary-bundle models has been proposed to describe capillary conductivity. In this work, we focus on the
50 models, which derive the pore-size distribution from the capillary water retention function and use the law of Hagen-Poiseuille and some assumptions about connectivity and tortuosity to predict hydraulic conductivity. We restrict the analysis to the prominent models of Childs and Collis-George (1950), Burdine (1953), Mualem (1976a) and Alexander and Skaggs (1986). As pointed out by Peters et al. (2023), these models are traditionally used to predict the *relative* conductivity, (i.e., the shape of the $K(h)$ relationship) from the WRC and scale it with a measured matching point, most often the measured
55 saturated conductivity (K_s). The models of Burdine (1953) and Alexander and Skaggs (1986) assume that the relative conductivity is derived from a simple bundle of continuous tortuous capillaries. To arrive at a simple mathematical expression, Alexander and Skaggs (1986) assumed that the tortuosity depends on both, the capillary saturation and pore radius.

Childs and Collis-George (1950) (CCG) proposed a more sophisticated statistical cut-and-random-rejoin-model. This model
60 was later enhanced by Mualem (1976a) through the incorporation of a correlation between pore length and pore diameter in the rejoined pore connections. Comprehensive overviews of the different model types can be found in Mualem and Dagan (1978), Mualem (1986), and Assoline and Or (2013). Although these different models are mentioned in numerous publications, generally only the model of Mualem (1976a) is used. An exception is the study conducted by Madi et al. (2018), who compared the capillary bundle models of Burdine (1953), Mualem (1976a), and Alexander and Skaggs (1986)
65 in terms of their applicability in predicting the relative hydraulic conductivity function. They found that the Alexander and



Skaggs model strongly overestimated the unsaturated conductivity for most soils, whereas the performances of the Burdine and Mualem models were reasonably good.

The aim of this study is to compare the capillary-bundle models of Childs and Collis-George (1950), Burdine (1953), Mualem (1976a) and Alexander and Skaggs (1986) with respect to their capability to fully predict hydraulic conductivity in the model framework outlined by Peters et al. (2023). To assess whether different WRC parametrization affect model performance, we combined four alternative frequently used unimodal capillary saturation models with the four different conductivity prediction models, leading to 16 model combinations for describing the SHP. All models were calibrated using 12 datasets that had sufficient information on the WRC and HCC for the calibration purpose. The predictive performance of the calibrated models was tested using 23 independent data sets with different soil textures.

75

2. Theory

Capillary bundle models have in common that they use a mathematical formulation of the capillary water retention function to express a porous medium's effective pore-size distribution. Applying the Hagen-Poiseuille law and some assumptions about pore connectivity and tortuosity, the models give mathematical descriptions of the hydraulic conductivity as function of matric suction, h [L], or water content, θ [L^3L^{-3}]. With few exceptions, the commonly used models predict a relative conductivity curve that needs to be scaled by matching it to one or more measured conductivity values to get the absolute HCC. We refer to Mualem and Dagan (1978), Mualem (1986) or Peters et al. (2023) for a thorough derivation of the capillary bundle models. In this study, we use the Peters-Durner-Iden (PDI) model system (Peters, 2013; 2014; Iden and Durner, 2014) to describe the WRC and HCC in the complete moisture range, because it accounts for capillary and non-capillary liquid storage and conductivity as well as vapor conductivity in a simple form and has proven its ability to well describe SHP data. A full description of the PDI model system is given in appendix A1. In the following, we only briefly review the capillary-bundle model formulations used in this study.

85

2.1 Tortuosity coefficient in capillary bundle models

A key role in any of the capillary-bundle models is played by the so-called tortuosity-connectivity correction, which differs between the various models proposed. It accounts in a lumped manner for a multitude of effects that distinguish a porous medium from a bundle of parallel tubes. The term tortuosity itself describes the effect that the path length for single water molecules, l_p , is longer than the direct projection distance l through the soil. Compared to water flow in straight capillaries, this leads to a reduction in the local conductivity caused by (i) a locally longer path and (ii) a locally smaller hydraulic gradient (Bear, 1972). The reduction of the effective hydraulic conductivity is then expressed by a tortuosity coefficient τ [-]:

90

$$\tau = \left(\frac{l}{l_p}\right)^2 \quad (1)$$



95 Note that τ is not a constant, but a function of capillary water content, since path length increases with decreasing water content. Furthermore, $\tau \neq 1$ at full water saturation because the flow path is always tortuous.

2.2 Relative capillary hydraulic conductivity prediction by capillary bundle models

The capillary bundle models are typically used to predict the relative capillary conductivity, K_{cr} [$L T^{-1}$] and need to be scaled by a scaling parameter, usually the saturated capillary conductivity, K_{cs} [$L T^{-1}$], leading to:

$$K_c = K_{sc} K_{cr} \quad (2)$$

100 where K_c [$L T^{-1}$] is the absolute capillary conductivity. Note that in the original works of Burdine (1953), Childs and Collis-George (1950), Mualem (1976a) and Alexander and Skaggs (1986), K_{sc} is identical to the total saturated conductivity K_s [$L T^{-1}$], whereas in the PDI scheme, K_s is given by the sum of saturated capillary and noncapillary conductivities (see appendix 1).

Burdine model (Bur)

105 Burdine (1953) suggested that relative conductivity of porous media can be described simply by the conductivity of a bundle of parallel tortuous capillaries of different size, where the tortuosity is inversely related to the capillary saturation leading to:

$$K_{rc} = S_c^2 \frac{\int_0^{S_c} h^{-2} d\tilde{S}_c}{\int_0^1 h^{-2} d\tilde{S}_c} \quad (3)$$

where \tilde{S}_c is the dummy variable of integration. The expression S_c^2 describes the dependence of the tortuosity correction on saturation S_c [-] ($0 < S_c < 1$).

Alexander and Skaggs (AS)

110 Alexander and Skaggs (1986) used a similar expression as Burdine (1953) but assumed that the tortuosity depends on the saturation and the pore radius by $l_p/l = C\sqrt{r/S_c}$ where C [$L^{-1/2}$] is a constant, which is not further specified, yielding:

$$K_{rc} = S_c \frac{\int_0^{S_c} h^{-1} d\tilde{S}_c}{\int_0^1 h^{-1} d\tilde{S}_c} \quad (4)$$

Note that the tortuosity correction is not solely given by S_c but is intrinsically given in the complete model by assuming that $l_p/l = C\sqrt{r/S_c}$.

Childs and Collis-George (CGG)

115 Childs and Collis-George (1950) developed a statistical cut-and-random-rejoin-model, which was further modified by Millington and Quirk (1961) and Kunze et al. (1968) and can be expressed in a general integral form by (Mualem, 1976a):

$$K_{rc} = S_c^\lambda \frac{\int_0^{S_c} (S_c - \vartheta) h^{-2} d\vartheta}{\int_0^1 (1 - \vartheta) h^{-2} d\vartheta} \quad (5)$$



where ϑ is a variable of integration, which represents the capillary saturation as function of h between the boundary limits, i.e. 0 and S_c (Mualem and Dagan, 1978). The tortuosity parameter λ [-] is 1 (Kunze et al., 1968) or 4/3 (Millington and Quirk, 1961).

120 **Mualem (Mual)**

Mualem (1976a) used the general approach of CCG and assumed that the length of a pore is directly proportional to its radius, which leads to:

$$K_{rc} = S_c^\lambda \left[\frac{\int_0^{S_c} h^{-1} d\tilde{S}_c}{\int_0^1 h^{-1} d\tilde{S}_c} \right]^2 \quad (6)$$

Applying his model to a variety of data, Mualem found empirically that $\lambda \approx 0.5$.

We may classify these four models into two groups, (i) relatively simple capillary bundle models (namely the Burdine and the AS model), which assume a bundle of parallel capillaries with tortuous flow paths, and (ii) two more sophisticated statistical cut-and-random-rejoin-models (namely the CCG and the Mualem model). Note that the tortuosity correction S_c^λ in these models becomes unity at saturation because it describes only the relative tortuosity reduction in drying soils.

2.3 Absolute capillary hydraulic conductivity prediction

Peters et al. (2023) (in the remainder “P23”) reformulated the capillary bundle model of Mualem (1976a) to predict absolute capillary conductivity. In a first step, they expressed the saturation-dependent absolute tortuosity coefficient τ [-] as the product of a relative tortuosity coefficient τ_r [-] ($0 < \tau_r < 1$) and a saturated tortuosity coefficient (τ_s) [-]:

$$\tau(S_c) = \tau_s \tau_r(S_c). \quad (7)$$

If we use Mualem's original expression for the relative tortuosity coefficient, $\tau_r = S_c^{0.5}$, the absolute conductivity prediction model reads (P23):

$$K_c = \beta \tau_s S_c^{0.5} (\theta_s - \theta_r)^2 \left[\int_0^{S_c} h^{-1} dS_c \right]^2 \quad (8)$$

where τ_s [-] is the saturated tortuosity coefficient. The coefficient $\beta = \sigma^2 / (2\eta\rho g)$ [$L^3 T^{-1}$] lumps all physical constants originating from the laws of Hagen-Poiseuille and Young-Laplace, where ρ [$M L^{-3}$] is the fluid density, g [$L T^{-2}$] is gravitational acceleration, η [$M L^{-1} T^{-1}$] is dynamic viscosity and σ [$M T^{-2}$] is the surface tension between the fluid and gas phases. The values of the physical constants used in this study are summarized in Tab. 1. If we use SI units, $\beta = 3.04 \times 10^{-4} m^3 s^{-1}$. If we use cm as length unit and d as time unit, $\beta = 2.62 \times 10^7 cm^3 d^{-1}$.



Table 1: Physical constants at 20°C used in this study.

Parameter	Definition	Unit	value
σ	Surface tension between fluid and gas phase	N m ⁻¹	0.0725
η	Dynamic viscosity of the bulk liquid	N s m ²	8.90×10^{-4}
ρ	Density of pure water at 298.15 K	kg m ⁻³	997.04
g	Gravitational acceleration constant	m s ⁻²	9.81

140

In essence, τ_s is the scaling parameter for the conductivity function in Eq. (7), as opposed to K_s in traditional prediction models. The underlying hypothesis is that the saturated tortuosity coefficient, unlike K_s , is subject to only moderate variations in soil and sample characteristics. Using the Fredlund and Xing (1994) saturation model within the PDI system as model for capillary water retention and Eq. (7) for the capillary conductivity function, P23 confirmed this hypothesis and found that τ_s has an average value of about 0.095 for soils differing greatly in their texture.

145

In P23, the analysis was restricted to the capillary bundle model of Mualem (Mual). In this paper, we apply the approach of P23 also to the capillary bundle models of Childs and Collis-George (CCG), Burdine (Bur), and Alexander and Skaggs (AS). This leads to the expressions listed in Tab. 2. For the complete derivation of the Burdine, CCG and Mualem models, we refer to Mualem and Dagan (1978). As mentioned above, for the AS model, the relative tortuosity is not solely given by S_c but is intrinsically given in the model by assuming that $l_p/l = C\sqrt{r/S_c}$. Thus, τ_s is given by $1/C^2$ and has the dimension L, and the parameter β is replaced by $\beta' = \sigma/4\eta$. With the values in Tab. 1, $\beta' = 20.4 \text{ m s}^{-1}$, resp. $\beta' = 1.76 \times 10^8 \text{ cm d}^{-1}$.

150

Table 2: Summary of the four prediction models for capillary hydraulic conductivity.

Name	prediction model for K_c	
Mual	$\beta\tau_s S_c^{0.5} (\theta_s - \theta_r)^2 \left[\int_0^{S_c} h^{-1} dS_c \right]^2$	(8)
CCG	$2\beta\tau_s S_c^{4/3} (\theta_s - \theta_r) \int_0^{S_c} (S_c - \vartheta) h^{-2} d\vartheta$	(9)
Bur	$\beta\tau_s S_c^2 (\theta_s - \theta_r) \int_0^{S_c} h^{-2} dS_c$	(10)
AS	$\beta'\tau_s S_c (\theta_s - \theta_r) \int_0^{S_c} h^{-1} dS_c$	(11)



155 3. Materials and Methods

3.1 Model combinations

To represent the complete SHP, we combined the four different capillary bundle models (Tab. 2) for the conductivity prediction with four basic capillary saturation functions (Tab. 3) within the PDI model system, leading to a total of 16 SHP models. The chosen saturation functions are the van Genuchten (1980) saturation function with (vGc) and without (vGmn) the constraint $m = 1 - 1/n$ (Tab. 3), the Kosugi (1996) saturation function (Kos), and the saturation function of Fredlund and Xing (1994) (FX). We selected these functions because they are the most commonly used unimodal saturation functions in the field of soil physics and geotechnics.

In each of the 16 model combinations, the relative tortuosity parameter λ was set to the original proposed values of $\lambda = 4/3$ for the CCG model, $\lambda = 2.0$ for the Burdine model, $\lambda = 0.5$ for the Mualem model, and $\lambda = 1.0$ for the AS model.

165

Table 3: Summary of the four capillary saturation functions. The parameters α , n , m , σ_{kos} , and h_m are shape parameters and e is the Euler number. These functions are scaled between 0 and 1 within the PDI scheme by Eq. (A.2).

Name	Basic capillary saturation function $S_c(h)$	
Kos	$\frac{1}{2} \operatorname{erfc} \left[\frac{\ln \left(\frac{h}{h_m} \right)}{\sqrt{2} \sigma_{kos}} \right]$	(12)
vGc	$\left(\frac{1}{1 + (\alpha h)^n} \right)^{1-1/n}$	(13)
vGmn	$\left(\frac{1}{1 + (\alpha h)^n} \right)^m$	(14)
FX	$\left(\frac{1}{\ln[e + (\alpha h)^n]} \right)^m$	(15)

Capillary bundle models can lead to unrealistic drops in the HCC close to water saturation, if the pore-size distribution underlying the WRC is wide (e.g., Vogel et al., 2001, Ippisch et al., 2006, Madi et al., 2018). To prevent such unrealistic decreases of $K(h)$, we applied the “hclip” approach of Iden et al. (2015). In this approach, an upper bound is assumed for the pore sizes that enter the calculations of the pore-bundle models. This is equivalent to setting a smallest value of suction h (h_{crit}) in the prediction integrals (8) to (11). Following Jarvis (2007) we assumed the maximum equivalent pore diameter of 0.5 mm, corresponding to $h_{\text{crit}} = 0.06$ m.

175 Since there exist no analytical solutions for several of the model combinations with respect to the capillary conductivity functions, we solved the integrals of the capillary conductivity functions (Tab. 2) by means of numerical integration using the trapezoidal method.



3.2 Calibration of τ_s for each model

For each of the 16 model combinations, a model-specific τ_s was determined by fitting the WRC and HCC models to measured data. The adjustable parameters were all WRC parameters and τ_s . For the non-capillary conductivity, which becomes important in the medium to dry range where film and corner flow is dominant, we used the prediction model of Peters et al. (2021). To obtain reliable estimates for τ_s , (i) data on the water retention function and (ii) hydraulic conductivity data in the wet range, but not at saturation, are required in high quality. We used the same 12 data sets that were already used by P23. The data encompass a wide variety of soil textures, from a pure sand to a clay loam. Details about the soils are given in the original literature and are summarized in Tab. 4.

Models were fitted to the data by nonlinear, weighted least squares regression. The objective function was

$$\phi(\mathbf{b}) = w_\theta \sum_{i=1}^{n_\theta} [\theta_i - \tilde{\theta}_i(\mathbf{b})]^2 + w_K \sum_{i=1}^{n_K} [\log_{10}(K_i) - \log_{10}(\tilde{K}_i(\mathbf{b}))]^2. \quad (16)$$

Here, θ_i and $\tilde{\theta}_i$ are the measured and modeled water contents, K_i and \tilde{K}_i are measured and modeled hydraulic conductivities, n_θ and n_K are the respective number of data points, $w_\theta = 10000$ and $w_K = 16$ are weights for the two data groups (Peters, 2011) and \mathbf{b} is the vector of unknown model parameters. The SCE-UA algorithm (Duan et al., 1992), was applied to minimize the objective function. Details can be found in P23. Model performance was quantified by the root mean squared errors (RMSE) of volumetric water content (WRC) and common log of $K(h)$ (HCC).

Table 4: SHP data used for model fitting.

Data set ID	Data set name in original publication	Source	Texture Class
Cal 1	Rehovot Sand	Mualem (1976b)	Sand
Cal 2	Gilat Loam		Loam
Cal 3	Pachapa Fine Sandy Clay (PFSC)		Sandy Clay
Cal 4	-	Pachepsky et al. (1984)	Sandy Loam
Cal 5	-		Silt Loam
Cal 6	-		Clay Loam
Cal 7	GG first sample	Sarkar et al. (2019)	Silt Loam
Cal 8	GG second sample		Silt Loam
Cal 9	JKI first sample		Loamy Sand
Cal 10	JKI second sample		Loamy Sand
Cal 11	SAU first sample		Sand
Cal 12	SAU second sample		Sand

3.3 Testing the predictive performance of the models

The prediction performance of the various model schemes was tested by comparing purely predicted HCC functions with measured conductivity data. For this test, we used the same 23 validation data sets as P23. Details about the data is given in Tab. 5. The test data comprise again a broad range of different texture classes. To describe the water retention data, the PDI retention model with the four basic saturation functions given in Tab. 3 were fitted. The conductivity functions were



200 predicted with model-specific values for τ_s as determined in the calibration. For the validation, the weight w_K in the objective function Eq. (16) was set to 0, so that the estimated parameter vector included only the WRC parameters.

Table 5: Data sets used to test the conductivity predictions.

Data set ID	Data set name in original publication	Source	Texture Class
Test 1*	-	Peters et al. (2023)	Silt Loam
Test 2*	-		Sandy Loam
Test 3*	-		Sandy Loam
Test 4	-		Sand
Test 5	-		Sandy Loam
Test 6	-		Loamy Sand
Test 7	-		Loamy Sand
Test 8	-		Sand
Test 9	-		Sand
Test 10	-		Loamy Sand
Test 11	-		Loamy Sand
Test 12**	coarse sand	Peters et. al. (2019)	Sand
Test 13	sand 1	Schelle et al. (2013)	Sand
Test 14	silt loam 1		Silt Loam
Test 15	sand 2a		Sand
Test 16*	silt loam 2		Silt Loam
Test 17*	sand 2b		Sand
Test 18*	silt		Silt
Test 19*	GG	Kirste et al. (2019)	Silt Loam
Test 20*	JKI		Sandy Loam
Test 21*	SAU		Sand
Test 22	HEB		Silt Loam
Test 23	SEL		Silty Clay Loam

* samples taken at same sites but different years as some of the calibration data (Cal7 to Cal 12)

** disturbed sample

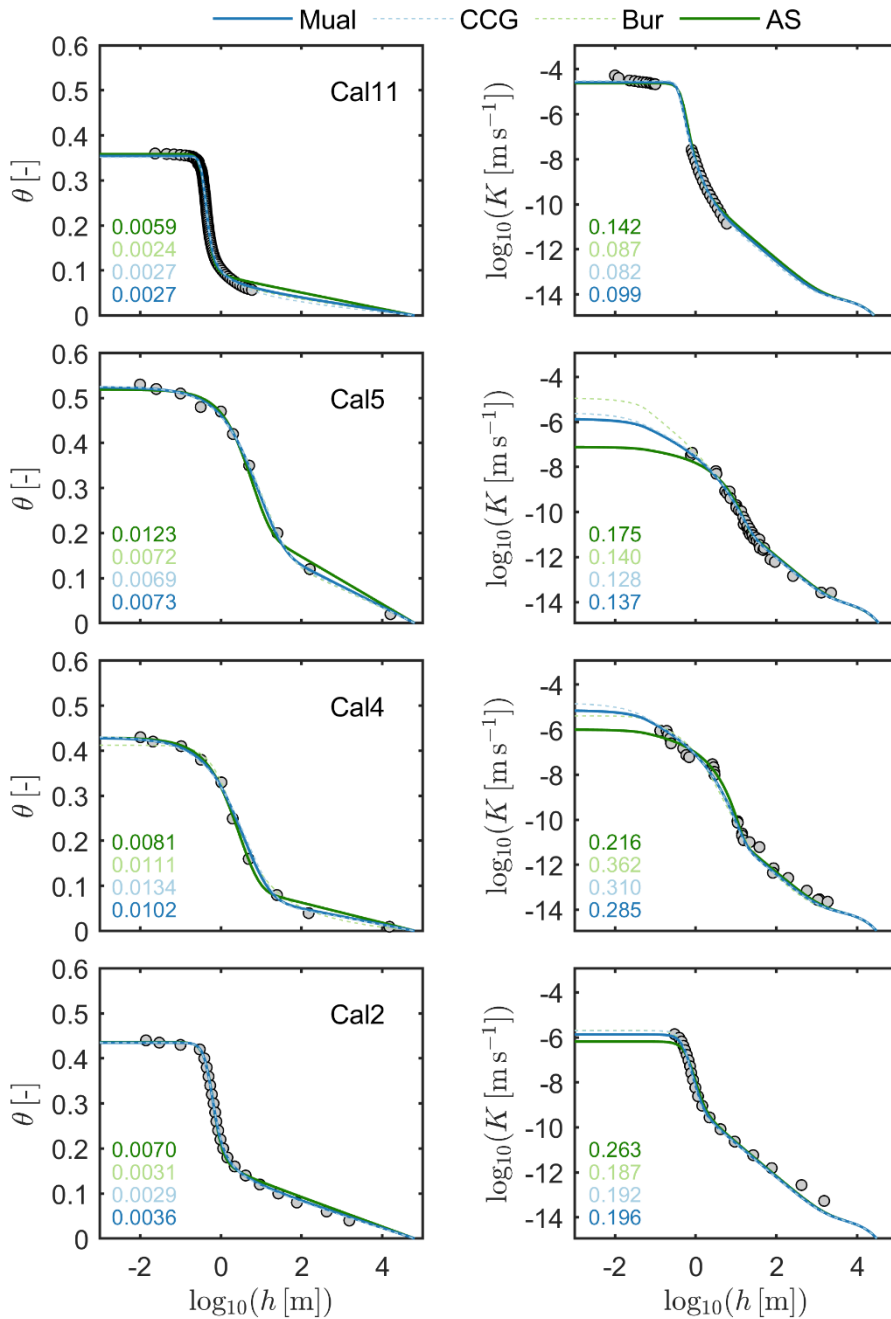
205 4. Results

4.1 Model-specific τ_s for the 16 model combinations

210 Figure 1 shows 4 out of the 12 calibration data sets together with the fitted retention curves in combination with the 4 conductivity models. We chose the FX-PDI model as saturation function for illustration since P23 found that it performed best in describing the retention data. However, the differences between different WRC models and the associated conductivity curves are small (see supplementary material). We limit Fig. 1 to four soils in order to keep the presentation concise; the corresponding graphs for all soils and all 16 model combinations are given in the supplementary material. Figure 2 shows the boxplots of the goodness-of-fit (RMSE) for all 12 calibration sets, and Fig. 3 depicts the boxplots of the model-specific optimal τ_s values.

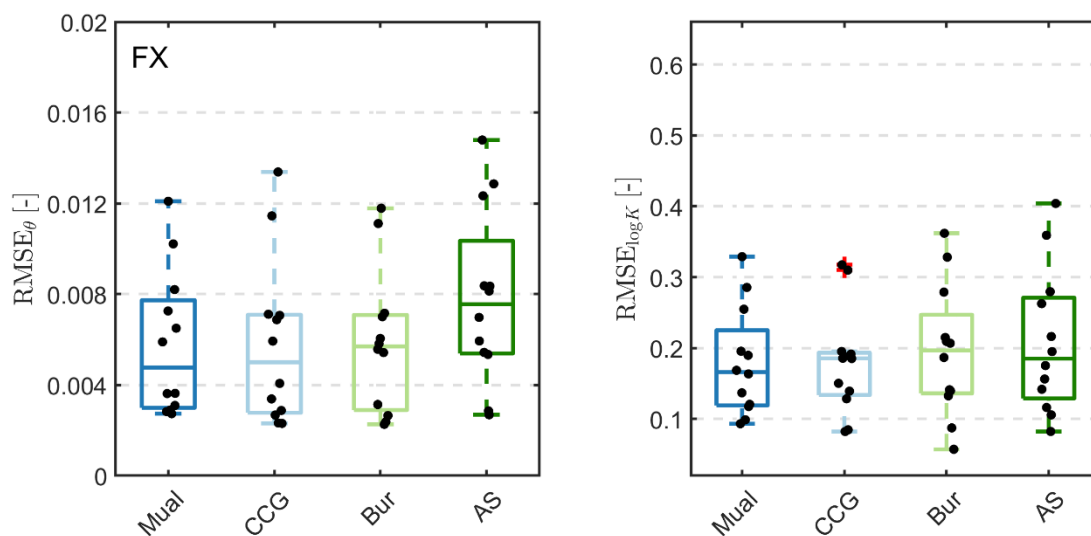


215 The goodness-of-fit for the 4 models is quantified by the $RMSE_{\theta}$ and $RMSE_{\log K}$ (Fig.2). The cut-and-random-rejoin models proposed by Mualem and CCG give rather small RMSE for the retention as well as the conductivity curves, whereas the conceptually simpler models of Burdine and AS perform less well. Specifically, the AS model could often describe the conductivity data adequately only at the expense of a poorer fit of the WRC data. Figure A1 shows the $RMSE_{\theta}$ and $RMSE_{\log K}$ boxplots for all 16 model combinations, revealing that the specific findings for the FX basic function can be generalized.



220

Figure 1: Plots of 4 of the 12 calibration data sets together with the fitted SHP functions. The FX-PDI model was used for WRC and four capillary bundle models were used for the HCC. The estimated parameters were the five parameters of the FX-PDI and the saturated tortuosity coefficient τ_s . The numbers in the subplots indicate RMSE $_{\theta}$ and RMSE $_{\log K}$ values for the four models.



225

Figure 2: Distributions of $RMSE_{\theta}$ and $RMSE_{\log K}$ when fitting the FX-PDI retention model in combination with the four capillary conductivity functions listed in Tab. 2 to the 12 calibration data sets. Black dots indicate single realizations. The red cross indicates an outlier, defined by the Matlab® default settings as 1.5 times the inter quartile range away from the top or bottom of the box (<https://de.mathworks.com/help/matlab/ref/boxchart.html>).

230 Figure 3 shows that the different conductivity prediction models give different optimal values for the saturated tortuosity coefficient. The median values for τ_s are 0.095 for the Mualem model, 0.27 for CCG, 0.014 for Burdine, and 7.8×10^{-5} for the AS model if the SWRC is described by the FX-PDI function. The values vary within a range of approximately 1.5 orders of magnitude for the Mualem and CCG models, slightly less than 2 orders of magnitude for the Burdine model, and more than 2 orders of magnitude for the AS model. The systematic differences of τ_s between the capillary bundle models can be

235 attributed to the differing conceptual approaches implicit to these models, as the physical parameters of fluid properties are consistent, and the functional representation of the effective pore-size distribution was the same. We note that models based on Mualem and CCG result in quite similar τ_s values whereas those of the Burdine model are a bit smaller. The AS model gives completely different values. Actually, the interpretation of τ_s in the AS model is difficult since part of the tortuosity is accounted for in the capillary model. Fig. A2 shows the distributions of the τ_s values for all 16 model combinations. The

240 medians of the estimated values for τ_s are summarized in Tab. 6.

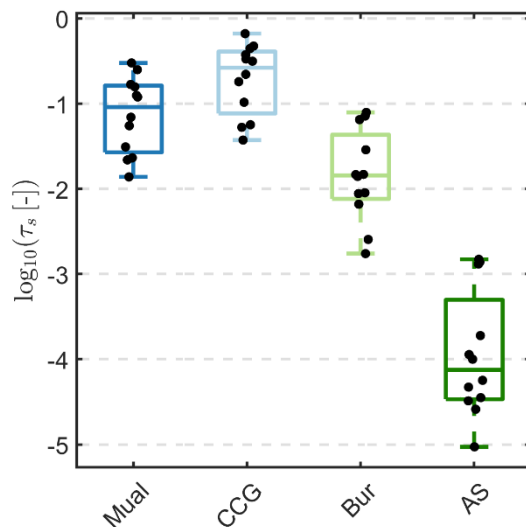


Figure 3: Distribution of optimal τ_s values obtained by fitting the four conductivity prediction models with the FX-PDI retention model to the 12 calibration data sets given in Tab. 4. Black dots indicate single realizations.

Table 6: Estimated values (median) of τ_s for all 16 model combinations.

	Mual	CCG	Bur	AS
Kos	0.084	0.230	0.011	7.7E-05
vGc	0.061	0.182	0.011	8.0E-05
vGmn	0.093	0.272	0.015	7.8E-05
FX	0.095	0.268	0.014	7.8E-05

245

4.2 Conductivity prediction accuracy by the different capillary bundle models

Fitting the retention models to the water retention data and using the values of τ_s obtained from the calibration (Tab. 6) we predicted the complete hydraulic conductivity functions for the 23 validation data sets and the 16 model combinations. Figure 4 shows the predicted functions and the data exemplarily for 6 out of the 23 data sets, again for the FX basic saturation model. With the exception of the AS model, the purely predicted conductivity curves agree remarkably well with the measured independent data. The curves for all data sets are given in the supplementary material.

250

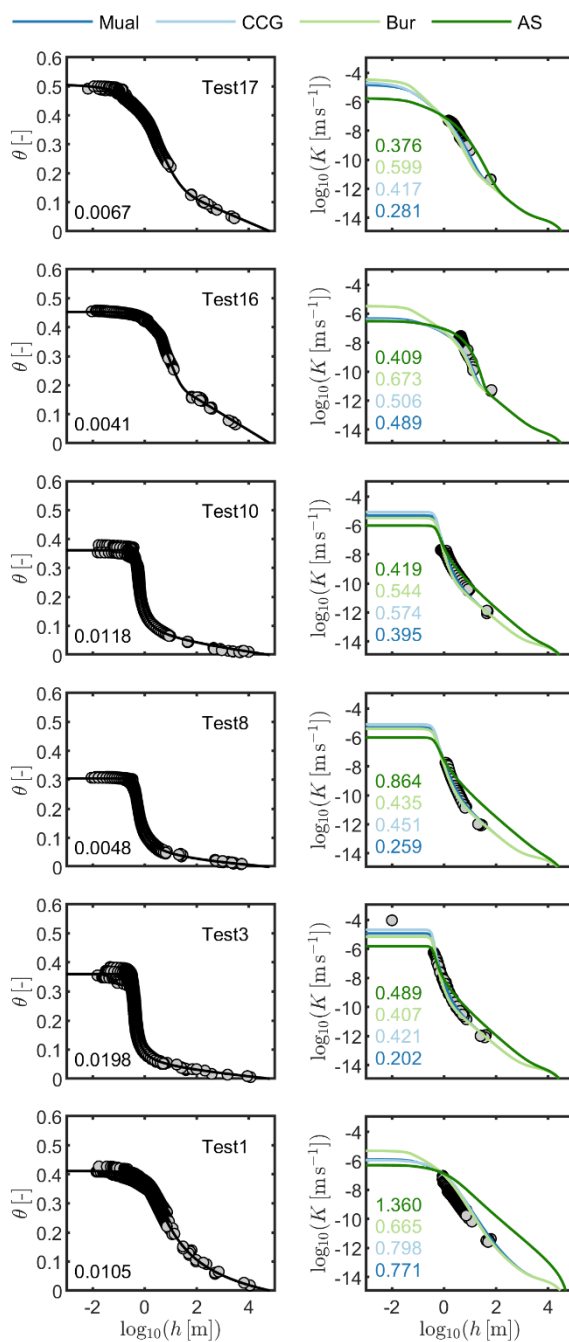


Figure 4: Measured data (dots), fitted retention functions (left) and predicted conductivity functions (right). Shown are 6 randomly selected soils out of 23 validation data sets. Numbers in the subplots indicate the RMSE_θ for the FX-PDI WRC model and the RMSE_{logK} values for the AS, Bur, CCG and Mual conductivity models, from top to bottom. Note that the conductivity curves are purely predicted and not fitted to the data.

255



Figure 5 shows the accuracy of the conductivity predictions again for the FX-PDI retention model, expressed by boxplots of the $RMSE_{\log K}$ and the mean error ($ME_{\log K}$). The distributions for all 16 model combinations are shown in Fig. A3. The median $RMSE_{\log K}$ in Fig. 5 is 0.40 for the Mualem model, which yields the best prediction of all 16 model schemes. For the CCG model the $RMSE_{\log K}$ is 0.42, for the Burdine model it is 0.44. For the AS model it is worst with a median of 0.66. Also, the AS model leads to the largest variation in the prediction accuracy.

For all 16 model combinations (Fig. A3), the Mualem model performed best for any of the investigated retention models. Table 7 lists the median $RMSE_{\log K}$ for all 16 model combinations. With the exception of the prediction that is based on the FX-PDI model, the median accuracy of the AS is as good or even better than the CCG and the Burdine model. However, the AS prediction accuracy shows for any WRC model a large spread of $RMSE_{\log K}$ with values up to 1.4 (Fig. 5; Fig. A3), which corresponds to a mismatch by a factor 25 in the K value. Contrary, the Mualem model performs not only well with respect to the median values but yields also the lowest spread for the $RMSE_{\log K}$ for any of the saturation functions, in other words it is the most robust. Figure 5 (right) and Fig. A3 indicate furthermore that only the combination of the FX capillary saturation function with the Mualem capillary bundle model leads to unbiased results. Summarizing the above findings, the preferred model combination is the basic FX saturation model with Mualem’s capillary conductivity model and $\tau_s = 0.095$.

The somewhat non-robust performance of the AS model, also found by Madi et al. (2018), can be explained by its assumption regarding tortuosity. We analyze this assumption in more detail in appendix A 3.

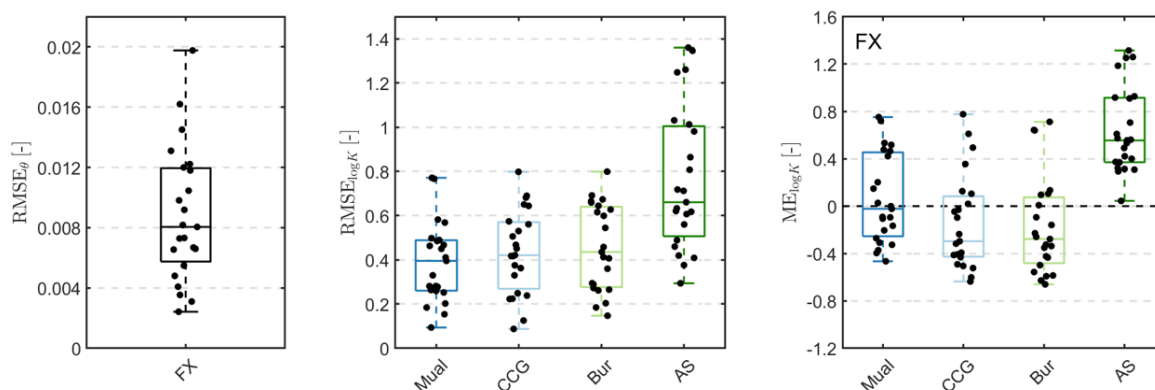


Figure 5: Left: $RMSE_{\theta}$ of the fitted PDI-FX retention model for the 23 test data sets. Center and right: $RMSE_{\log K}$ and mean errors of the predicted absolute conductivities by the four models listed in Table 2. Black dots indicate single realizations.



Table 7: Median of $RMSE_{\log K}$ for all model combinations.

	Mual	CCG	Bur	AS
Kos	0.69	0.79	0.81	0.74
vGc	0.64	0.73	0.78	0.66
vGmn	0.48	0.60	0.65	0.45
FX	0.40	0.42	0.44	0.66

4.3 Behavior of the capillary bundle models in the wet range

285 In the very wet moisture range, even tiny changes in the WRC can have a large impact on the HCC. Such small changes at
arbitrary small suctions occur in common WRC parameterizations for soils with wide pore-size distributions or for bimodal
soils. Durner (1994) concluded accordingly three decades ago that this makes a conductivity prediction based on statistical
pore-bundle models in the range close to full saturation virtually impossible. In Fig. 6, we evaluate this effect for the 4
different conductivity prediction models. For illustration, we use the rather fine textured silt loam (calibration data set 5) and
290 show all model fits with and without consideration of a maximum pore-size in the capillary bundle models (“hclip”, Iden et
al., 2015), as described in section 3.1.

In all cases, we fitted the retention model parameters and τ_s to the data. The fitted retention curves (FX-PDI) lie almost on
top of each other (again with a slight difference for the AS model, as discussed in section 4.3). The four conductivity models
fit the given data similarly well, but show a very different behavior in wet moisture range, where no data are available. All
295 models with the exception of the AS model show in the “unclipped” version (dashed lines) a strong increase of conductivity
in the pressure range close to saturation, from about $h < 0.01$ m. This illustrates the artifact of using capillary bundle-models
without limiting the maximum pore size in the integrals used to calculate the conductivity function and is the reason for
introducing a maximum pore-size in the integration. In a classic approach where the relative conductivity function is
predicted and matched to a measured or assumed value for K_s , the unsaturated conductivity curve would be accordingly
300 dramatically underestimated. The AS model appears to be least affected by this artifact.

However, even if the change of the HCC close to saturation caused by this artifact is removed, the four models differ
markedly in their predicted shape in the moderately moist region (Fig. 6, “with clipping”; solid lines). The differences
between the 4 models reach still almost 2 orders of magnitude and they develop in a suction range where we are still far from
unrealistically large pores sizes (recall that in the “hclip curves”, the maximum allowed pore diameter was 0.5 mm,
305 corresponding to a suction of 0.06 m).

The reason for the varying behavior lied in the distinct pore-bundle models utilized. The Burdine model, which assumes that
the pore paths are parallel and tortuous, yields the greatest conductivity increase for large pores due to the Hagen-Poiseuille
relationship with pore size. In contrast, the CCG and Mualem models, which involve cutting and randomly rejoining most of



the direct paths, mitigate this effect and exhibit comparable patterns. The AS model seems to underestimate the conductivity
310 increase.

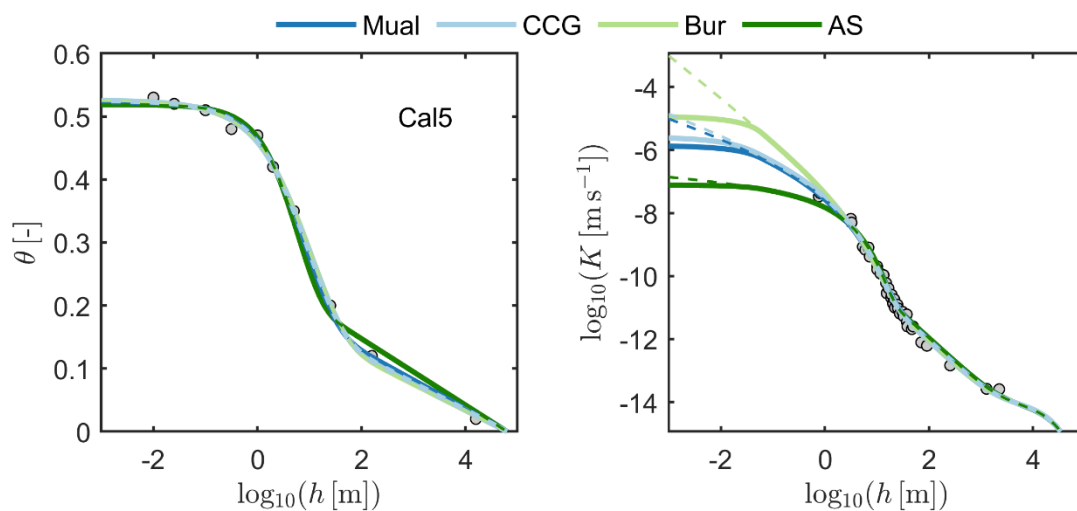


Figure 6: Fitted retention and conductivity functions with and without “hclip” to calibration set Cal 5. Solid lines: with clipping; dashed lines: without clipping. Basic capillary saturation function is the FX model.

5. Summary and conclusion

315 In this study we compared 4 different capillary bundle models in combination with 4 different unimodal capillary saturation models, leading to 16 model combinations, to predict the absolute hydraulic conductivity within the PDI model framework. For each of the 16 model combinations, we determined a model-specific value for the saturated tortuosity coefficient τ_s by fitting the models to a calibration data set. Using these general values of τ_s , we then predicted for independent data sets all three components of conductivity, namely isothermal vapor, non-capillary and capillary liquid conductivity from the WRC
320 without any adjusted parameters, following Peters et al. (2021; 2023).

When predicting the HCC from the WRC, a good representation of water retention function is essential; therefore, the best performing model schemes were those that used the flexible 3-parameter capillary saturation functions in the WRC model (i.e., the Fredlund and Xing (1994) model and the unconstrained van Genuchten (1980) model with independent parameters m and n).

325 Among the capillary bundle models, the cut-and-random rejoin models introduced by Childs and Collis-George (1950) and Mualem (1976a) exhibited the best performance, with the Mualem model performing slightly superior. The Burdine (1953) model was less suited, while the model of Alexander and Skaggs (1986) cannot be recommended due to its unphysical representation of the relative tortuosity. Since the model of Mualem (1976a) is mathematically simpler than the model of Childs and Collis-George (1950), we conclude that its establishment in soil hydrology is justified. The median $RMSE_{\log K}$



330 was 0.4 for the recommended FX-PDI-Mualem combination. In other words, the median uncertainty of the predicted K is about a factor of 2.6, which is quite fair in the light of the expected measurement uncertainties.

Interestingly, the different models show, even when fitted to data, a quite different behavior close to saturation if extrapolated. We explain this with the different model structure. Especially the Burdine model overestimates the conductivity increase caused by the consideration of even small amounts of water in large pores, since the law of Hagen-
335 Poiseuille is directly applied to a certain pore diameter as derived from the water retention characteristics. In the two cut-and-random-rejoin models the combination of pores of different sizes leads to a much smaller conductivity contribution of that water in the largest pores. The AS model seems to underestimate the conductivity increase in the wet range.

Our approach for estimating conductivity refers solely on the conductivity of the soil matrix, without considering the impact of soil structure. The prediction can be useful in situations where no conductivity data are available. In cases where a
340 measured value of the saturated conductivity (K_s) is available and soil structure is a significant factor (which is typically the case for most topsoils), combining the predicted hydraulic conductivity curve (HCC) with an interpolation towards K_s can provide a well-defined conductivity function over the entire moisture range, as outlined by P23. By distinguishing between structural and textural effects, this approach ensures a physically consistent use of measured SHP information

Appendix

345 A 1. The PDI Model System

A 1.1. PDI Water Retention Function

The capillary saturation function S_c [-] and a non-capillary saturation function S_{nc} [-] may be superposed in the form (Peters, 2013; Iden and Durner, 2014):

$$\theta(h) = (\theta_s - \theta_r)S_c + \theta_r S_{nc}. \quad (\text{A.1})$$

350 in which the first right term holds for water stored in capillaries, and the second term for water stored in adsorbed water films and pore corners, θ [$\text{m}^3 \text{m}^{-3}$] is the total water content, h [m] is the suction head and θ_s [$\text{m}^3 \text{m}^{-3}$] and θ_r [$\text{m}^3 \text{m}^{-3}$] are the saturated and maximum adsorbed water contents, respectively. To meet the physical requirement that the capillary saturation function reaches zero at oven dryness, a basic saturation function $\Gamma(h)$ is scaled by (Iden and Durner, 2014):

$$S_c(h) = \frac{\Gamma(h) - \Gamma(h_0)}{1 - \Gamma(h_0)}, \quad (\text{A.2})$$

355 with h_0 [m] being the suction head at oven dryness, which can be set at $10^{4.8}$ m following Schneider and Goss (2012). $\Gamma(h)$ can be any uni- or multi-modal saturation function such as the unimodal functions of van Genuchten (1980) and Kosugi (1996), or their bimodal versions (Durner, 1994; Romano et al., 2011).



The saturation function for non-capillary water is given by a smoothed piecewise linear function (Iden and Durner, 2014), which is here given in the notation of Peters et al. (2021):

$$360 \quad S_{nc}(h) = \frac{\ln\left(\frac{h_0}{h}\right) - b \ln\left(1 + \left[\frac{h_a}{h}\right]^{1/b}\right)}{\ln\left(\frac{h_0}{h_a}\right)}, \quad (\text{A.3})$$

in which the parameter h_a [m] reflects the suction head where non-capillary water reaches its saturation (fixed in our study to the suction at which capillary saturation reaches 0.75). The derivation for h_a as a quantile of S_c is given in Peters et al. (2023) and the resulting mathematical expressions are listed appendix A.1.3. The parameter h_0 in Equation (A.3) is the suction head where the water content reaches zero, which reflects the suction at oven-dry conditions. $S_{nc}(h)$ increases
 365 linearly from zero at oven dryness to its maximum value of 1.0 at h_a , and then remains constant toward saturation. In order to ensure a continuously differentiable water capacity function, $S_{nc}(h)$ must be smoothed around h_a , which is achieved by the smoothing parameter b [-] (Iden and Durner, 2014), given here by:

$$b = b_o \left(1 + 2 \frac{1 - e^{-b_1}}{n^2}\right), \quad (\text{A.4})$$

where $b_o = 0.1 \ln(10)$ and $b_1 = \left(\frac{\theta_r}{\theta_s - \theta_r}\right)^2$.

370 A 1.2. PDI Hydraulic Conductivity

The PDI hydraulic conductivity model is expressed as (Peters et al., 2013):

$$K(h) = K_c + K_{nc} + K_v, \quad (\text{A.5})$$

where K_c [-] [m s^{-1}], K_{nc} [m s^{-1}], and K_v [m s^{-1}] are the conductivities for the capillary, non-capillary and isothermal vapor conductivities respectively. K_{nc} is given by (Peters et al., 2021):

$$375 \quad K_{nc} = c \theta_m h_a^{-1.5} \left(\frac{h_0}{h_a}\right)^{-1.5(1 - S_{nc})}, \quad (\text{A.6})$$

in which c is used to account for several physical and geometrical constants and can be either a free fitting parameter to scale K_{nc} or $c = 1.35 \times 10^{-8} \text{ m}^{5/2} \text{ s}^{-1}$. Parameter θ_m [-] is the water content at $h = 10^3$ m. We refer to Saito et al. (2006) or Peters (2013) for details regarding the formulation of K_v as a function of the invoked WRC. The conductivity for water flow in capillaries is in this paper described using the 4 pore bundle models summarized in Tab. 2.



380 **A 1.3. Calculation of h_a**

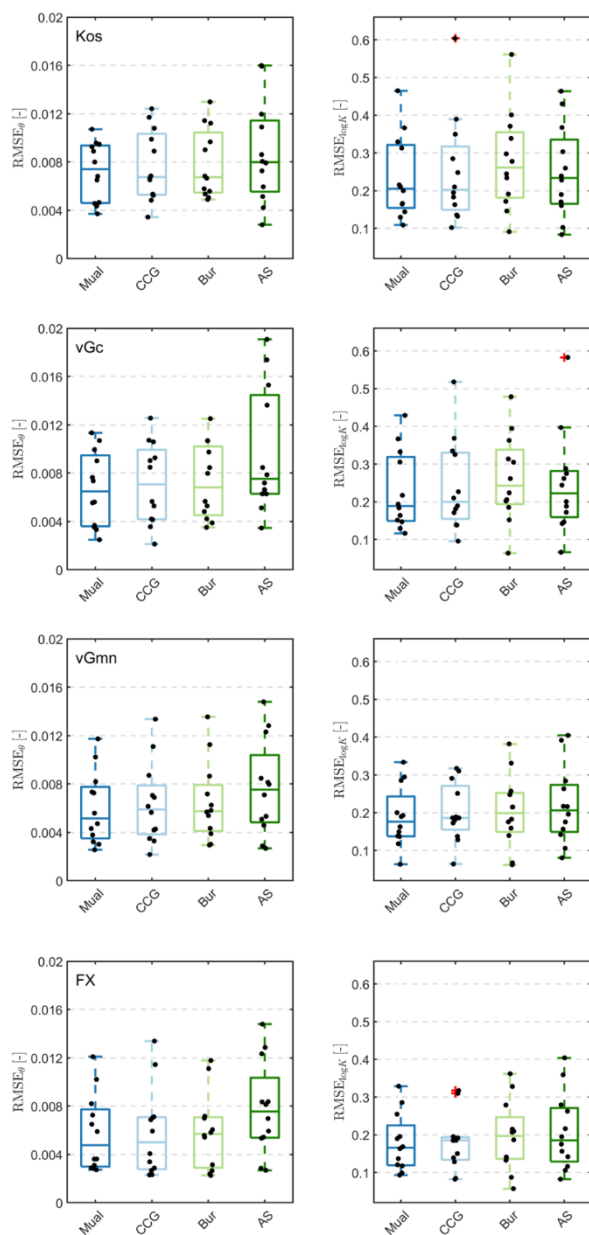
According to Peters et al. (2023), we set the air entry parameter for the non-capillary parts of the hydraulic functions, h_a to the suction at which capillary saturation reaches 0.75. The expressions for the used capillary saturation functions are summarized in Tab A 1.

385 **Table A1:** Mathematical expressions for h_a for the used capillary saturation functions as derived by Peters et al. (2023). The parameter γ is given by $\gamma = \xi(1 - F_0) + F_0$.

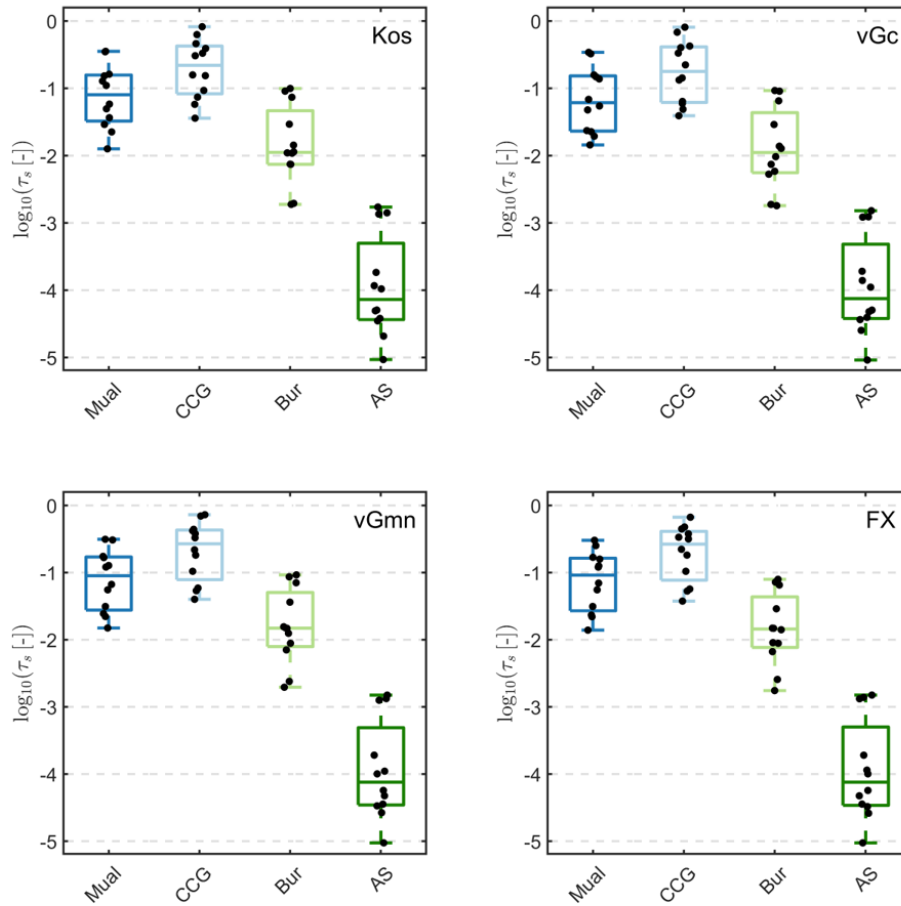
Name	Mathematical expressions for h_a
Kos	$h_m e^{\sqrt{2} \sigma \operatorname{erfc}^{-1}(2\gamma)}$
vGc and vGmn	$\alpha^{-1} \left[\gamma^{-\frac{1}{m}} - 1 \right]^{1/n}$
FX	$\alpha^{-1} \left(\exp\left(\gamma^{-\frac{1}{m}}\right) - e \right)^{\frac{1}{n}}$



A 2. Results for all model combinations



390 **Figure A1:** Distributions of $RMSE_{\theta}$ and $RMSE_{\log K}$ when fitting the 4 retention model in combination with the four capillary
 conductivity functions listed in Tab. 2 and Tab. 3 to the 12 calibration data sets. 1st row: Kos as basic saturation function; 2nd
 row: vGc as basic saturation function; 3rd row: vGmn as basic saturation function; 4th row: FX as basic saturation function.
 Black dots indicate single realizations. The red crosses indicate outliers, defined by the Matlab® default settings as 1.5 times
 the inter quartile range away from the top or bottom of the box (<https://de.mathworks.com/help/matlab/ref/boxchart.html>).
 395



400 **Figure A2:** Distribution of fitted τ_s values for the 4 different capillary bundle models and the 4 basic capillary saturation functions fitted to the 12 data sets (see Fig. 6) given in Tab. 4. Black dots indicate single realizations. Top, left: Kos as basic saturation function; Top, right: vGc as basic saturation function; Bottom, left: vGmn as basic saturation function; Bottom, right: FX as basic saturation function.

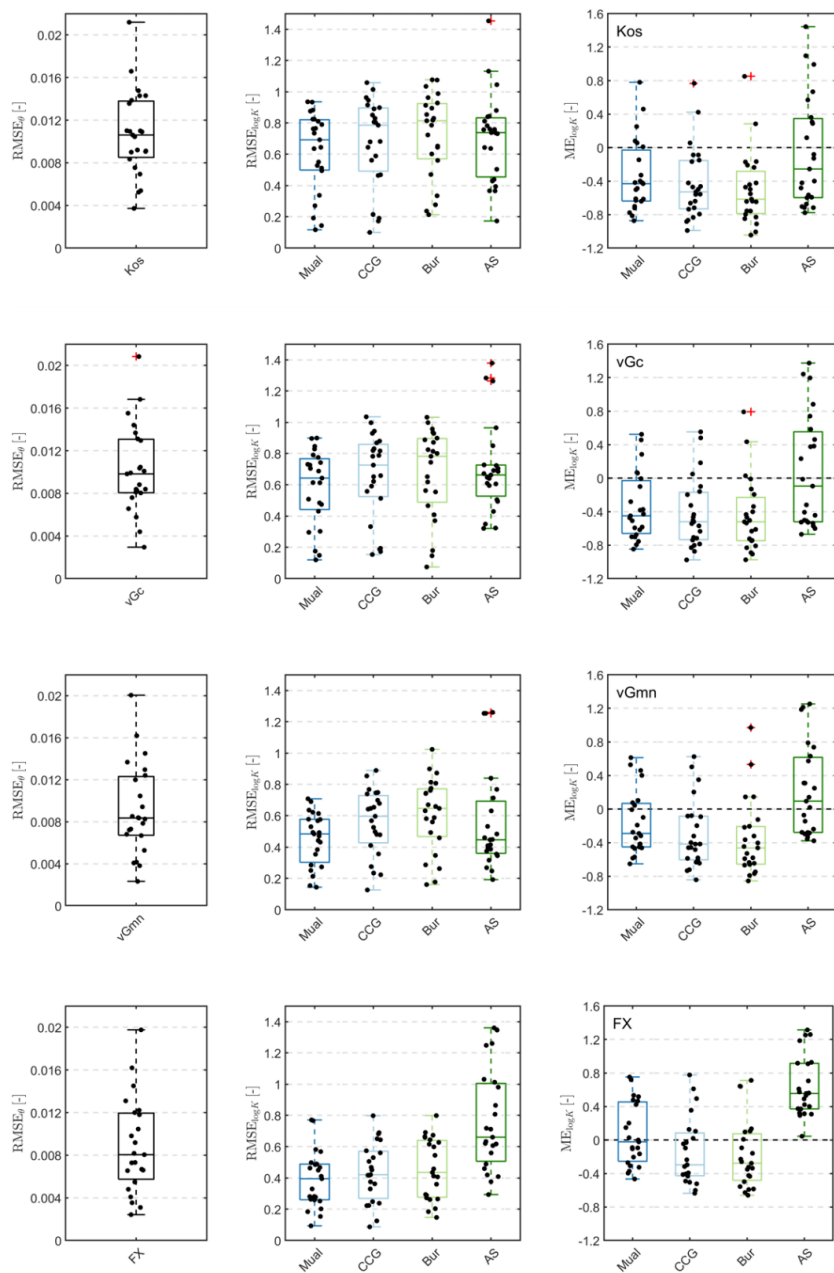


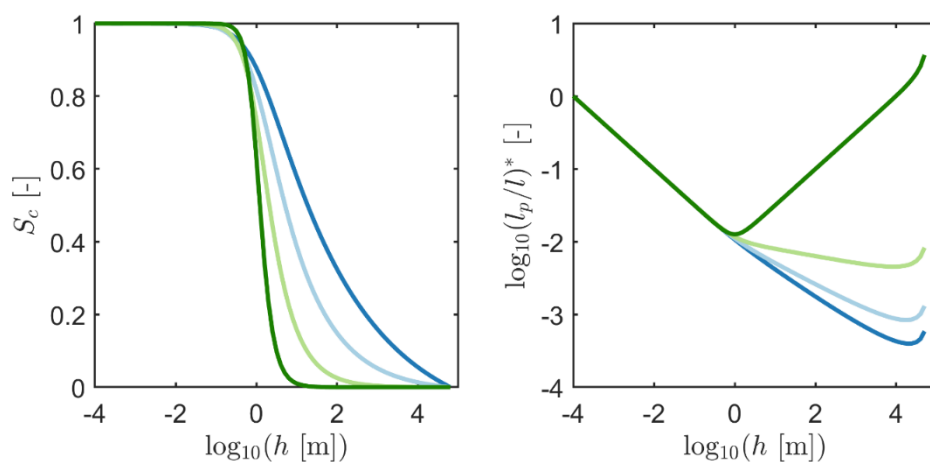
Figure A3: Left: $RMSE_{\theta}$ of the fitted PDI retention models for the 23 test data sets. Center and right: $RMSE_{\log K}$ and mean errors of the predicted absolute conductivities for all 4 different capillary bundle models and the 4 basic capillary saturation functions listed in Tab. 2 and 3. Black dots indicate single realizations. 1st row: Kos as basic saturation function; 2nd row: vGc as basic saturation function; 3rd row: vGmn as basic saturation function; 4th row: FX as basic saturation function. The red crosses indicate outliers, defined by the Matlab® default settings as 1.5 times the inter quartile range away from the top or bottom of the box (<https://de.mathworks.com/help/matlab/ref/boxchart.html>).



A 3. Analyzing the tortuosity assumption of Alexander and Skaggs (1986)

410 Physically, the path elongation due to tortuosity l_p/l should strictly increase with decreasing saturation. In the AS model it is assumed to follow $l_p/l = C\sqrt{r/S_c}$. Figure 7 visualizes the relationship between tortuosity and pressure head for four different capillary saturation functions, which reflect differently wide pore-size distributions. The path elongation l_p/l , plotted as relative function $(l_p/l)^*$, decreases with increasing h (decreasing saturation) which is unphysical. The only exception is found for the very narrow pore-size distribution in the range beyond the air-entry point. When fitting

415 simultaneously the WRC and HCC, this behavior of the AS conceptual model is counteracted by a worse fit of the retention data (see Figs. 1 and 2). In a pure prediction, where only the retention model is fitted, this can lead to a bad performance of the conductivity prediction. Similar to our results, Madi et al. (2018), who used the measured saturated conductivity for scaling, found that the AS model severely overestimates the unsaturated conductivity for most soils.



420 **Figure A4:** Scaled tortuosity correction used by AS conductivity prediction model for soils with different pore-size distributions. Left: Capillary saturation functions using the vGc saturation function with $\alpha = 1.0 \text{ m}^{-1}$ and n varying from 1.2 to 4.0. Right: associated scaled tortuosity correction $l_p/l = C\sqrt{r/S_c}$. Since we are only interested in the general shape of the function, we scaled l_p/l by assuming $C = 1$ and dividing it by its value at $h = 10^{-4} \text{ m}$.



425 **Data availability:** The calibration data sets Cal 1 to Cal 6 cannot be provided due to copyright restrictions (Cal 1 to Cal 3: Mualem (1976b); Cal 4 to Cal 6: Pachepsky et al. (1984)). The other six calibration data sets and all test data sets are given in the supplemental material S2.

Acknowledgments: This study was financially supported by the Deutsche Forschungsgemeinschaft (DFG grant PE 1912/4-1).

430 **Author contributions:** Conceptualization: AP; model implementation and analysis: AP; draft preparation and discussions: AP, SCI, and WD.

Competing interests: The contact author has declared that none of the authors has any competing interests.

References

- 435 Alexander, L., and Skaggs, R. W.: Predicting unsaturated hydraulic conductivity from the soil water characteristic. *Transactions of the ASAE*, 29(1), 176-184, doi: 10.13031/2013.30123, 1986.
- Assouline, S. and Or, D.: Conceptual and parametric representation of soil hydraulic properties: A review, *Vadose Zone J.*, 12, 1–20, <https://doi.org/10.2136/vzj2013.07.0121>, 2013.
- Bear, J.: *Dynamics of Fluids in Porous Media*, Elsevier, New York, ISBN 0486131807, 1972.
- 440 Burdine, N.: Relative permeability calculations from pore size distribution data, *J. Petrol. Technol.*, 5, 71–78, 1953.
- Childs, E. C. and Collis-George, N.: The permeability of porous materials, *Proc. R. Soc. Lon. Ser.-A*, 201, 392–405, 1950.
- Duan, Q., Sorooshian, S., and Gupta, V.: Effective and efficient global optimization for conceptual rainfall-runoff models, *Water Resour. Res.*, 28, 1015–1031, 1992.
- Durner, W.: Hydraulic conductivity estimation for soils with heterogeneous pore structure, *Water Resour. Res.*, 30, 211–222, 445 <https://doi.org/10.1029/93WR02676>, 1994.
- Fredlund, D. G. and Xing, A. Q.: Equations for the soil water characteristic curve, *Can. Geotech. J.*, 31, 521–532, <https://doi.org/10.1139/t94-061>, 1994.
- Iden, S. and Durner, W.: Comment on “Simple consistent models for water retention and hydraulic conductivity in the complete moisture range” by A. Peters, *Water Resour. Res.*, 50, 7530–7534, <https://doi.org/10.1002/2014WR015937>, 2014.



- 450 Iden, S. C., Peters, A., and Durner, W.: Improving prediction of hydraulic conductivity by constraining capillary bundle models to a maximum pore size, *Adv. Water Resour.*, 85, 86–92, 2015.
- Ippisch, O., Vogel, H.-J., and Bastian, P.: Validity limits for the van Genuchten–Mualem model and implications for parameter estimation and numerical simulation, *Adv. Water Resour.*, 29, 1780–1789, 2006.
- Jarvis, N. J.: A review of non-equilibrium water flow and solute transport in soil macropores: Principles, controlling factors and consequences for water quality, *Eur. J. Soil. Sci.*, 58, 523–546, 2007.
- 455 Kosugi, K.: Lognormal distribution model for unsaturated soil hydraulic properties, *Water Resour. Res.*, 32, 2697–2703, 1996.
- Kunze, R. J., Uehara, G., and Graham, K.: Factors important in the calculation of hydraulic conductivity, *Soil Sci. Soc. Am. J.*, 32, 760–765, 1968.
- 460 Lebeau, M. and Konrad, J.-M.: A new capillary and thin film flow model for predicting the hydraulic conductivity of unsaturated porous media, *Water Resour. Res.*, 46, W12554, <https://doi.org/10.1029/2010WR009092>, 2010.
- Madi, R., de Rooij, G. H., Mielenz, H., and Mai, J.: Parametric soil water retention models: a critical evaluation of expressions for the full moisture range, *Hydrol. Earth Syst. Sci.*, 22, 1193–1219, <https://doi.org/10.5194/hess-22-1193-2018>, 2018.
- 465 Millington, R. J. and Quirk, J. P.: Permeability of porous solids, *T. Faraday Soc.*, 57, 1200–1207, 1961.
- Mualem, Y.: A new model for predicting the hydraulic conductivity of unsaturated porous media, *Water Resour. Res.*, 12, 513–522, 1976a.
- Mualem, Y.: A catalog of the hydraulic properties of unsaturated soils (Tech. Rep), Technion – Israel Institute of Technology, 1976b.
- 470 Mualem, Y.: Hydraulic conductivity of unsaturated soils: Prediction and formulas, *Methods of Soil Analysis: Part 1 Physical and Mineralogical Methods*, 5, 799–822, <https://doi.org/10.2136/sssabookser5.1.2ed.c31>, 1986.
- Mualem, Y., and Dagan, G.: Hydraulic conductivity of soils: Unified approach to the statistical models. *Soil Science Society of America Journal*, 42(3), 392–395, <https://doi.org/10.2136/sssaj1978.03615995004200030003x>, 1978.
- Pachepsky, Y., Scherbakov, R., Varallyay, G., and Rajkai, K.: On obtaining soil hydraulic conductivity curves from water retention curves, *Pochvovedenie*, 10, 60–72, 1984 (in Russian).
- 475 Peters, A.: Simple consistent models for water retention and hydraulic conductivity in the complete moisture range, *Water Resour. Res.*, 49, 6765–6780, <https://doi.org/10.1002/wrcr.20548>, 2013.



- Peters, A.: Reply to comment by S. Iden and W. Durner on “Simple consistent models for water retention and hydraulic conductivity in the complete moisture range”, *Water Resour. Res.*, 50, 7535–7539, <https://doi.org/10.1002/2014WR016107>,
480 2014.
- Peters, A. and Durner, W.: A simple model for describing hydraulic conductivity in unsaturated porous media accounting for film and capillary flow, *Water Resour. Res.*, 44, W11417, <https://doi.org/10.1029/2008WR007136>, 2008.
- Peters, A. and Durner, W.: Reply to comment by N. Shokri and D. Or on “A simple model for describing hydraulic conductivity in unsaturated porous media accounting for film and capillary flow”, *Water Resour. Res.*, 46, W06802,
485 <https://doi.org/10.1029/2010WR009181>, 2010.
- Peters, A., Durner, W., and Wessolek, G.: Consistent parameter constraints for soil hydraulic functions, *Adv. Water Resour.*, 34, 1352–1365, 2011.
- Peters, A., Iden, S. C., and Durner, W.: Local Solute Sinks and Sources Cause Erroneous Dispersion Fluxes in Transport Simulations with the Convection–Dispersion Equation, *Vadose Zone J.*, 18, 190064,
490 <https://doi.org/10.2136/vzj2019.06.0064>, 2019.
- Peters, A., Hohenbrink, T. L., Iden, S. C., and Durner, W.: A simple model to predict hydraulic conductivity in medium to dry soil from the water retention curve, *Water Resour. Res.*, 57, e2020WR029211, <https://doi.org/10.1029/2020WR029211>, 2021.
- Peters, A., Hohenbrink, T. L., Iden, S. C., van Genuchten, M. Th., and Durner, W.: Prediction of the absolute hydraulic
495 conductivity function from soil water retention data, *Hydrol. Earth Syst. Sci.*, 27, 1565–1582, <https://doi.org/10.5194/hess-27-1565-2023>, 2023.
- Romano, N., Nasta, P., Severino, G., and Hopmans, J. W.: Using Bimodal Lognormal Functions to Describe Soil Hydraulic Properties, *Soil Sci. Soc. Am. J.*, 75, 468–480, <https://doi.org/10.2136/sssaj2010.0084>, 2011.
- Saito, H., Šimunek, J., and Mohanty, B. P.: Numerical analysis of coupled water, vapor, and heat transport in the vadose
500 zone, *Vadose Zone J.*, 5, 784–800, 2006.
- Sarkar, S., Germer, K., Maity, R., and Durner, W.: Measuring near-saturated hydraulic conductivity of soils by quasi unit-gradient percolation – 2. Application of the methodology, *J. Plant Nutr. Soil Sc.*, 182, 535–540, <https://doi.org/10.1002/jpln.201800383>, 2019.
- Schelle, H., Heise, L., Jänicke, K., and Durner, W.: Water retention characteristics of soils over the whole moisture range: A
505 comparison of laboratory methods, *Eur. J. Soil. Sci.*, 64, 814–821, 2013.
- Schneider, M. and Goss, K.-U.: Prediction of the water sorption isotherm in air dry soils, *Geoderma*, 170, 64–69, <https://doi.org/10.1016/j.geoderma.2011.10.008>, 2012.



Tuller, M. and Or, D.: Hydraulic conductivity of variably saturated porous media: Film and corner flow in angular pore space, *Water Resour. Res.*, 37, 1257–1276, <https://doi.org/10.1029/2000WR900328>, 2001.

510 Tokunaga, T. K.: Hydraulic properties of adsorbed water films in unsaturated porous media, *Water Resour. Res.*, 45, W06415, <https://doi.org/10.1029/2009WR007734>, 2009.

van Genuchten, M. Th.: A closed-form equation for predicting the hydraulic conductivity of unsaturated soils, *Soil Sci. Soc. Am. J.*, 44, 892–898, 1980.

515 Vogel, T., Van Genuchten, M. T., and Cislérova, M.: Effect of the shape of the soil hydraulic functions near saturation on variably-saturated flow predictions, *Adv. Water Resour.*, 24, 133–144, 2000.

Zhang, Z. F.: Soil water retention and relative permeability for conditions from oven-dry to full saturation, *Vadose Zone J.*, 10, 1299–1308, <https://doi.org/10.2136/vzj2011.0019>, 2011.